Spontaneous emergence of large scale cell cycle synchronization in amoeba colonies

SUPPLEMENTARY INFORMATION

Igor Segota, Laurent Boulet, David Franck & Carl Franck

Laboratory of Atomic and Solid State Physics, Cornell University, Ithaca, NY 14853, USA

1. Probability distribution of phase coherence *r* for *N* random oscillators

We start by representing the size (area) of each cell by a unit vector with length $L = 1$ in complex plane $e^{i\theta_j}$ where j is the cell index. The probability distribution of each step is then:

$$p(\vec{r}_j) = p(r_j, \theta_j) = \frac{1}{2\pi L}\delta(r_j - L)$$

which is normalized:

$$\int_{\theta_j=0}^{2\pi}\int_{r_j=0}^{\infty} p(r_j, \theta_j) r_j dr_j d\theta_j = \int_{\theta_j=0}^{2\pi}\int_{r_j=0}^{\infty} \frac{1}{2\pi L}\delta(r_j - L) r_j dr_j d\theta_j = 1$$

where $\delta(r_j - L)$ is the Dirac delta function. The average and variance of a single step are:

$$\langle \vec{r}_j \rangle = \int \vec{r}_j p(\vec{r}_j) d\vec{r}_j = L \cdot 0 = 0$$

$$\sigma_{rj}^2 = \langle {r_j}^2 \rangle = \int {r_j}^2 \frac{1}{2\pi L}\delta(r_j - L) 2\pi r_j dr_j = L^2$$

Also note that:

$$\sigma_{xj}^2 = \frac{1}{2}\sigma_{rj}^2 = \frac{L^2}{2}, \quad \sigma_{rj}^2 = \sigma_{xj}^2 + \sigma_{yj}^2$$

Now for the average:

$$\vec{z} = \frac{1}{N}\sum_{j=1}^{N}\vec{r}_j, \quad z_x = \frac{1}{N}\sum_{j=1}^{N} r_{xj}, \quad z_y = \frac{1}{N}\sum_{j=1}^{N} r_{yj}$$

we can apply Central Limit Theorem for each x and y component individually (if N is large). Each Cartesian component x and y (of z) then has a Normal distribution with mean 0 and variance $\sigma_{xj}^2/N = L^2/(2N)$. The probability distribution of z is:

$$p(z_x, z_y) = Ae^{-\frac{z_x^2}{2\sigma_{xj}^2/N}} e^{-\frac{z_y^2}{2\sigma_{yj}^2/N}} = Ae^{-\frac{(z_x^2+z_y^2)}{2\sigma_{xj}^2}} = Ae^{-\frac{r^2}{L^2/N}}$$

where the normalization constant can be obtained by requiring that the integral of this probability is 1 and we evaluate the integral in polar coordinates r, ψ:

$$\int_{\psi=0}^{2\pi}\int_{r=0}^{\infty} Ae^{-\frac{r^2}{L^2/N}} r d\psi dr = 1 = 2\pi A\frac{L^2}{2N} = \frac{A\pi L^2}{N}, \quad A = \frac{N}{\pi L^2}$$

The average phase coherence for a random system can be directly calculated:

$$\langle r\rangle = \int_{\psi=0}^{2\pi}\int_{r=0}^{\infty} \frac{N}{\pi L^2} e^{-\frac{r^2}{L^2/N}} r^2 d\psi dr = \frac{\sqrt{\pi}}{2}\frac{L}{\sqrt{N}}$$

and the average of r^2 is:

$$\langle r^2\rangle = \int_{\psi=0}^{2\pi}\int_{r=0}^{\infty} \frac{N}{\pi L^2} e^{-\frac{r^2}{L^2/N}} r^3 d\psi dr = \frac{L^2}{N}$$

so the variance is $\sigma_r^2 = \langle r^2\rangle - \langle r\rangle^2 = \frac{L^2}{N} - \frac{\pi}{4}\frac{L^2}{N}$ and the standard deviation is:

$$\sigma_r = \frac{L}{\sqrt{N}}\sqrt{\frac{4-\pi}{4}}$$

which gives us the relative fluctuation:

$$\frac{\sigma_r}{\langle r\rangle} = \frac{\sqrt{\frac{4-\pi}{4}}}{\frac{\sqrt{\pi}}{2}} = \sqrt{\frac{4}{\pi} - 1} \approx 0.52$$

In Fig.3 in the main text we make use of $\langle r\rangle$ and σ_r to show the average and the standard deviation for the phase coherence for finite populations.

2. Additional examples of cell synchronization

Here we show two more examples indicating an onset of synchronized growth (Fig. S1). The cell synchronization occurs very quickly, within the first several hours. These runs also reveal longer time behavior than in Fig. 3, indicating decay of coherence at long times (see discussion in the main text).

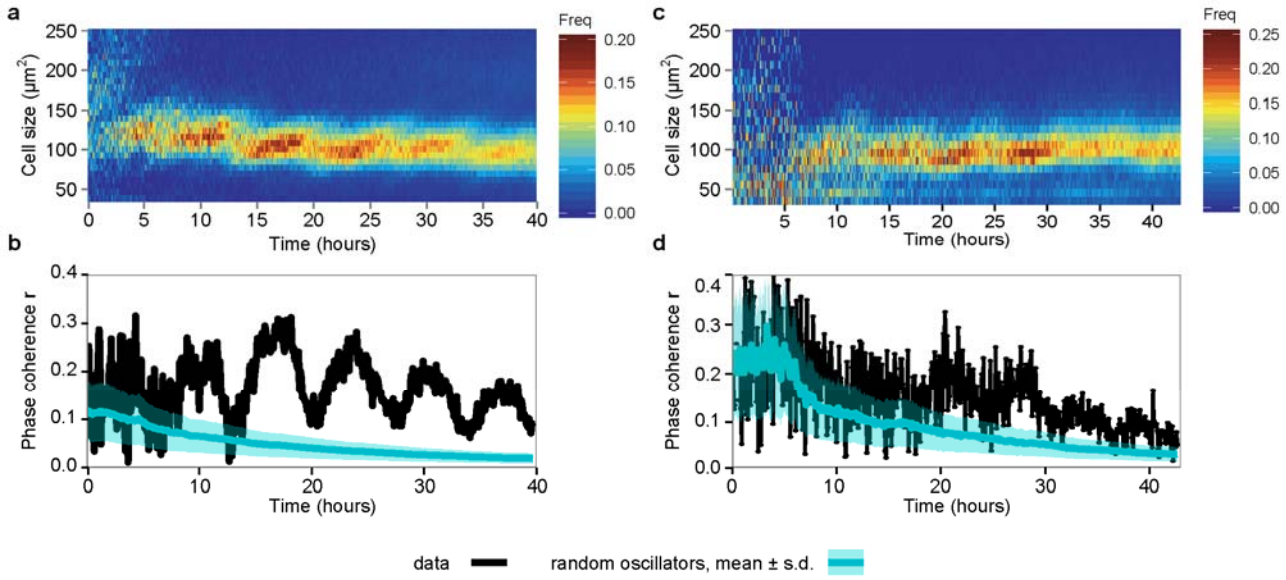

Figure S1. **Additional examples of cell synchronization.** The dynamics of cell size distribution and phase coherence for the first **(a,b)** and second **(c,d)** experiment. As in main text, black lines denote phase coherence in our data and cyan line and its spread shows the mean phase coherence and its spread for the corresponding number of randomly oscillating cells.

3. Statistical analysis of the number of cell divisions vs time

We analyzed the number of cell divisions for three experiments (Fig. S2a) by manually counting each cell division event, as described in the Results section of the main text. The experiments 1 and 3 were performed simultaneously on Olympus IX71 and Nikon Optiphot microscopes in brightfield, as detailed in the Methods section of the main text. Next, these distribution of cell divisions were smoothed using a local polynomial fit [1] (Fig. S2b) and then normalized by the total cell number. The cell densities were 14.5, 10 and 7.4 cells/mm^2, respectively. These smoothed distributions were then divided by the instantaneous cell density at each time point to obtain the relative number of cell divisions over one hour intervals $\Delta N/N$. This is shown in Fig. S3 together with the resulting mean and the corresponding standard error of the mean.

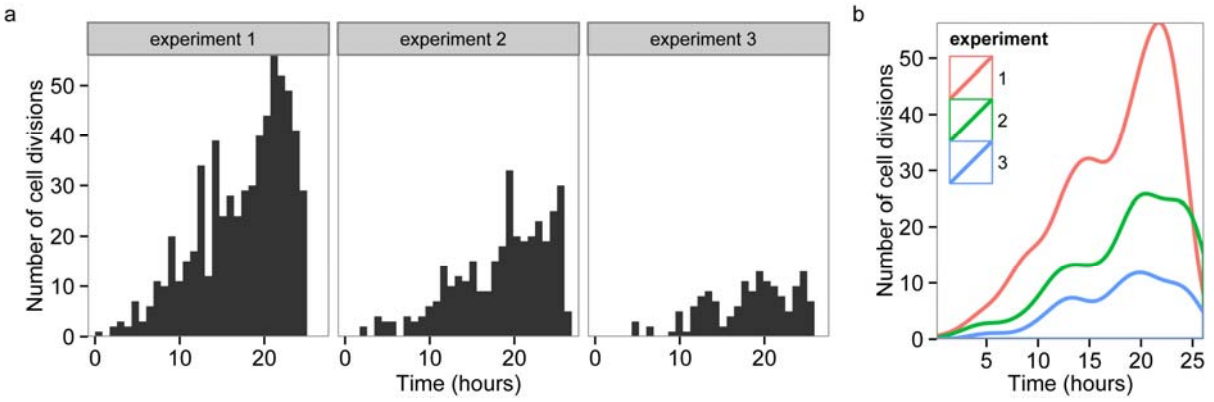

Figure S2. **Distribution of cell divisions vs time. a**, Histograms showing the number of cell divisions in 1 hour intervals from three different experiments. Experiments 1 and 3 were performed simultaneously. **b**, Smoothed distributions from **a** using local polynomial fits [1].

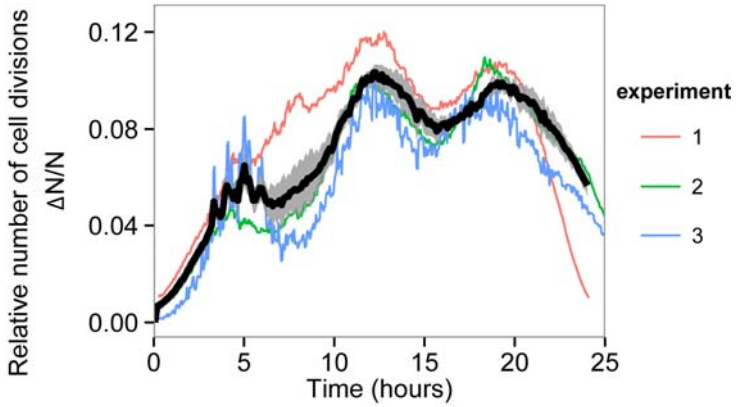

Figure S3. Relative number of cell divisions in one hour time intervals for three experiments (shown in red, green and blue) and its average (black) and standard error of the mean (gray spread).

4. Estimate of the variation of the degree of coherence with increasing number of cells

We can estimate of the effect of cell proliferation on the degree of cell cycle synchronization according to the Kuramoto model. Recent efforts to explore the phenomenon of synchronization of many oscillators have focused of extensions of the Kuramoto model to include explicit consideration of network topology, interaction strength and finite population. The problem at hand invites us to consider the last aspect: what are the dynamics of synchronization for a growing population? From [2], we have the following equation for r, long time coherence of the system:

$$r = \sum_{\{\omega\}} p(\omega) \left[1 - \left(\frac{\Delta(\omega)}{K\, r}\right)^2\right]^{1/2} \quad \text{(SI-1)}$$

where the summation is over a collection of N oscillators whose unperturbed frequencies are given by the set $\{\omega\}$, the probability of each value of frequency is given by $p(\omega)$, K is the interoscillator coupling strength in

the (infinitely-ranged) Kuramoto model (Eqn. 1 on p. 146 of) and $\Delta(\omega) \stackrel{\text{def}}{=} \omega - \langle\omega\rangle$ is the deviation of the frequency of a particular oscillator from the mean frequency of the entire set of oscillators,$\langle\omega\rangle$. We examine the dependence of r on N with a minimalist distribution: all the oscillators have either $\omega = \omega_0 + \delta$ or $\omega = \omega_0 - \delta$ with equal probability. Then we have the following equation for r:

$$r = \sum_{\{\omega\}} p(\omega)\left[1 - \left(\frac{\delta}{K\,r}\right)^2\right]^{1/2} = N\left(\frac{1}{N}\right)\left[1 - \left(\frac{\delta}{K\,r}\right)^2\right]^{1/2} = \left[1 - \left(\frac{\delta}{K\,r}\right)^2\right]^{1/2} \qquad \text{(SI-2)}$$

We conclude that r is independent of N. We therefore do not expect the degree of coherence achieved at long times to vary as the cells proliferate.

5. Peclet numbers

Following the discussion in [3] the Peclet number is the dimensionless number quantifying the ratio of advective to diffusive transport, defined as:

$$Pe = \frac{Lv}{D}$$

where L is a characteristic length of the flow cell, v is the advective flow speed and D is the diffusion coefficient of the particle being transported. In our analysis in the main text, we calculated the Peclet numbers for small molecules such as cAMP to give an estimate of the range of flow rates in the microfluidic experiments that could perturb chemical signaling through the intercellular medium.

6. Synchronization in monoclonal populations and lineage effects

We investigated the degree of phase coherence in monoclonal populations, starting from a 1 cell per 4 mm^2 area, which is the minimum cell surface density achievable in our experimental setup. The mean and standard deviation of doubling times owing to cell-to-cell variation were 7.3 ± 0.8 hours. We determined this based on the experiment presented in Fig. 1 in the main text by manually tracking 55 cells (Fig. S4).

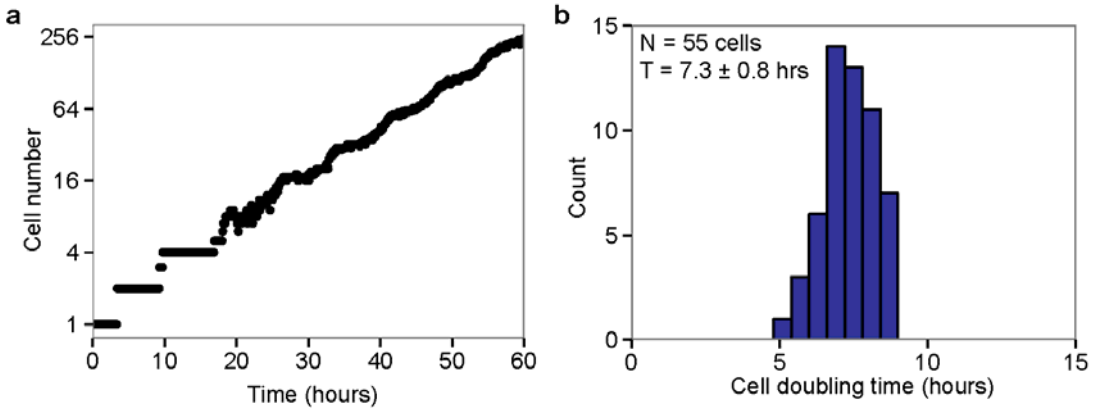

Figure S4. **Single cells growth. a,** Growth dynamics of single cell growth. **b,** Distribution of single cell doubling times showing cell-to-cell variability.

If the cell division is thought of as a random walk process with the mean $T_D = 7.3$ hours and standard deviation $\sigma = 0.8$ hours (assuming this is unchanged without coupling), we can estimate the number of generations needed for the complete loss of lineage effect. The number of generations n needed for the standard deviation $\sigma\sqrt{n}$ to become equal to the mean T_D is $n \approx 80$. This is due to the fact that the cell division clock is relatively precise with only about 10% error (Fig. S4b). The dynamics of cell size distribution and phase coherence for single-cell experiments are shown in Fig. S5 and, as expected, show a very strong lineage effect.

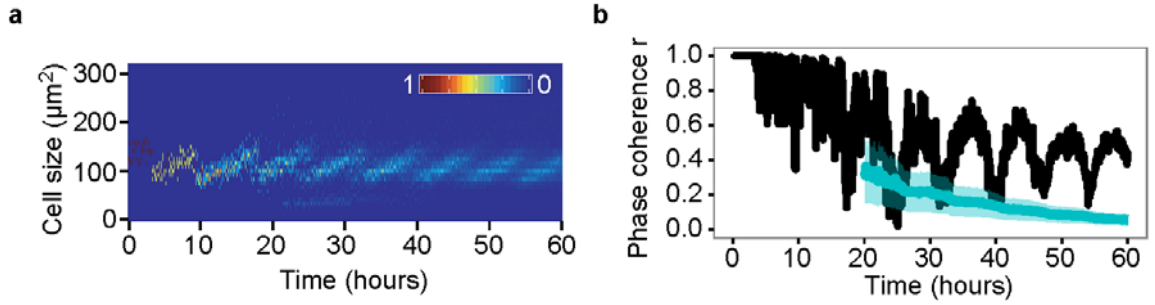

Figure S5. **Lineage effects in single cell growth. a,** Cell size distribution for a monoclonal population started from a single cell. **b,** Phase coherence for the same system showing the lineage effect. The cyan line and its spread denote the average and standard deviation for random-phase systems for large number of cells.

7. Shear stresses employed are well below the threshold for cellular response

We consider the shear stress on a cell modeled as a thin planar disk on the bottom of our microfluidic flow chamber. From [4] we expect that such time-independent low Reynolds number (i.e. friction dominated) flow can be approximated as Poiseuille channel flow as follows: We have velocity $u(y)\hat{x}$ in the horizontal (x) direction and velocity variation only along the vertical (y) driven by a constant pressure gradient $\frac{dP}{dx}$ according to:

$$\mu \frac{\partial^2 u}{\partial y^2} = \frac{dP}{dx}$$

where μ is the dynamic viscosity. Applying no slip boundary conditions at the top and bottom of the channel $u(y = 0) = 0, u(y = h) = 0$ where h is the height of the channel, gives us the solution for the velocity:

$$u(y) = \left(\frac{dP}{dx}\right)\frac{1}{2}y(y - h)$$

In our case the volumetric flow Q is experimentally fixed so we have (for channel width given by Δz)

$$Q = \Delta z \int_0^h \frac{dP}{dx}\frac{1}{2}y(y - h)dy = \left(-\frac{dP}{dx}\right)\frac{\Delta z \cdot h^3}{12}$$

The shear stress σ in our device near the wall is then (Eq. 1 in [4]) :

$$\sigma = \mu\left(\frac{\partial u}{\partial y}\right) = \frac{6Q\mu}{\Delta z \cdot h^2}$$

For our device [3] we have values $\Delta z = 1400\ \mu m$, $h = 200\ \mu m$ and $Q = 0.4\ \mu l/min$ as our maximum flow rate (for Peclet number ~10) and we used the dynamic viscosity of water at 25 C, $\mu = 0.894\ mPa \cdot s$ [5]. This gives us a maximum shear stress of $\sigma_{max} = 6.4 \cdot 10^{-4}\ Pa$.

Compared to typical shear stresses needed to induce cell motility and rearrangement of actin cytoskeleton in *Dictyostelium* of about 0.1-0.7 Pa [6] [7], the shear stresses in our experiments are well below these (more than two orders of magnitude). In endothelial cells, the lowest shear stresses needed to induce responses such as potassium channel activation or the rise of intracellular Ca^{2+} is on the range from 2×10^{-2} Pa to 1 Pa [8]. In the very worst case, the lowest recorded shear stress for these responses in endothelial cells is a factor of 30 greater than the highest shear stress in our experiments [9]. Therefore, it is very unlikely that the loss of cell cycle coherence observed here (Fig. 2e; main text) is due to shear stress.

8. Bibliography

1. Available at http://www.inside-r.org/r-doc/stats/loess (2013).

2. van Hemmen, J. L. & Wreszinski, W. F., Lyapunov Function for the Kuramoto Model of Nonlinearly Coupled Oscillators. *J. Stat. Phys.* **72**, 145-166 (1993).

3. Franck, C., Ip, W., Bae, A., Franck, N., Bogart, E. & Thi Le, T., Contact-mediated cell-assisted cell proliferation in a model eukaryotic single-cell organism: an explanation for the lag phase in shaken cell culture. *Phys Rev E* **77**, 041905 (2008).

4. Tritton, D. J., *Physical Fluid Dynamics* (Oxford University Press, New York, 1988).

5. Dortmund Data Bank, Available at http://www.ddbst.com/en/EED/PCP/VIS_C174.php (2013).

6. Decave, E., Rieu, D., Dalous, J., Fache, S., Brechet, Y., Fourcade, B., Satre, M. & Bruckert, F., Shear-flow induced motility of Dictyostelium discoideum cells on solid substrate. *J. Cell Sci.* **116**, 4331-4343 (2003).

7. Fache, S., Dalous, J., Engelund, M., Hansen, C., Chamaraux, F., Fourcade, B., Satre, M., Devreotes, P. & Bruckert, F., Calcium mobilization stimulates Dictyostelium discoideum shear-flow-induced cell motility. *J. Cell Sci.* **118**, 3445-3458 (2005).

8. Davies, P. F., Flow-mediated endothelial mechanotransduction. *Physiol. Rev.* **75**, 519-560 (1995).

9. Malek, A. M. & Izumo, S., Mechanism of endothelial cell shape change and cytoskeletal remodeling in

response to fluid shear stress. *J. Cell Sci.* **109**, 713-726 (1996).

10. De Monte, S., d'Ovidio, F. & Sorensen, P. G., Dynamical quorum sensing: Population density encoded in cellular dynamics. *PNAS* **104** (47), 18377–18381 (2007).

11. Loomis, W. F., *The Development Of Dictyostelium Discoideum* (Academic Press Inc., New York, 1982).